



IMPLICATIONS OF THE TEVATRON JET RESULTS ON PDF

LEVAN BABUKHADIA
FOR THE DØ COLLABORATION*Department of Physics, State University of New York
Stony Brook, NY 11794, USA
E-mail: blevan@fnal.gov*

We report a new measurement of the pseudorapidity (η) and transverse-energy (E_T) dependence of the inclusive jet production cross section in $p\bar{p}$ collisions at $\sqrt{s} = 1.8$ TeV using 95 pb^{-1} of data collected with the DØ detector at the Fermilab Tevatron. The differential cross section $d^2\sigma/(dE_T d\eta)$ is presented up to $|\eta| = 3$, significantly extending previous measurements. The results are in good overall agreement with next-to-leading order predictions from QCD, indicate a preference for certain parton distribution functions, and provide the world's best constraint on the gluon distribution at high parton momentum fraction x .

1 Introduction

This past decade has witnessed impressive progress in both the theoretical and experimental understanding of the collimated streams of particles or “jets” that emerge from inelastic hadron collisions. Theoretically, jet production in hadron collisions is understood within the framework of Quantum Chromodynamics (QCD), as a hard scattering of the constituent partons (quarks and gluons) that, having undergone a collision, manifest themselves as jets in the final state. QCD predicts the amplitudes for the hard scattering of partons at high momentum transfers. Perturbative QCD calculations of jet cross sections, ¹ using accurately determined parton distribution functions (PDFs), ² have increased the interest in jet measurements at the $\sqrt{s} = 1.8$ TeV Tevatron proton-antiproton collider. Consequently, the two Tevatron experiments, DØ and CDF, have served as prominent arenas for studying hadronic jets.

Here, we report a new measurement of the pseudorapidity (η) and transverse-energy (E_T) dependence of the inclusive jet production cross section, ³ which examines the short-range behavior of QCD, the structure of the proton in terms of PDFs, and possible substructure of quarks and gluons. We present the differential cross section $d^2\sigma/(dE_T d\eta)$ as a function of jet E_T in five intervals of η , up to $|\eta| = 3$, where the pseudorapidity is defined as $\eta = \ln[\cot(\theta/2)]$, with θ being the polar angle. The present measurement is based on 95 pb^{-1} of data collected with the DØ detector ⁴ during 1994–1995, and significantly extends previous measurements, ⁵ as indicated by the kinematic reach shown in Fig. 1a.

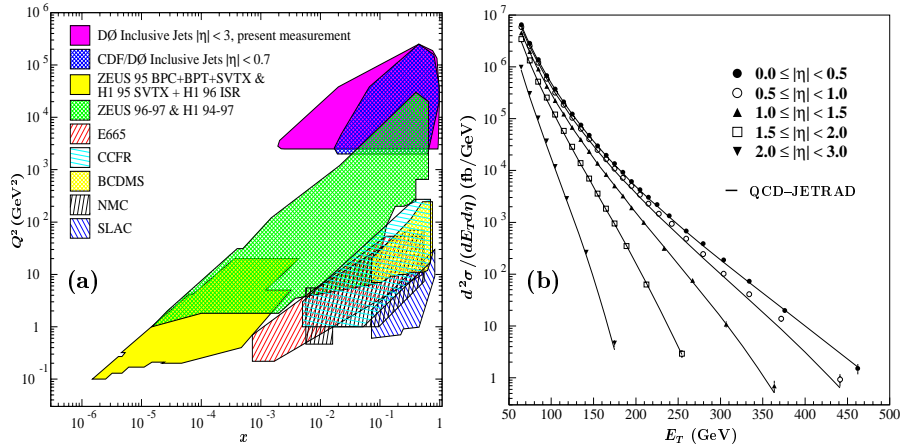


Figure 1. (a) The kinematic reach of this measurement along with that of other collider and fixed-target experiments in the plane of the parton momentum fraction x and the square of the momentum transfer Q^2 , and (b) the single inclusive jet production cross section as a function of jet E_T , in five pseudorapidity intervals, showing only statistical uncertainties, along with theoretical predictions.

2 Jet Definition and Experimental Systematics

Jets are reconstructed using an iterative cone algorithm with a fixed cone radius of $\mathcal{R} = 0.7$ in $\eta - \varphi$ space, where φ is the azimuth. Offline data selections eliminate contamination from background caused by electrons, photons, noise, or cosmic rays. This is achieved by applying an acceptance cutoff on the z -coordinate of the interaction vertex, flagging events with large missing transverse energy, and applying jet quality criteria. Details of data selection and corrections due to noise and/or contamination are described elsewhere.³ A correction for jet energy scale accounts for instrumental effects associated with calorimeter response, showering and noise, as well as for contributions from spectator partons, and corrects on average the reconstructed jet E_T to the “true” E_T .^{3,6} The effect of calorimeter resolution on jet cross section is removed through an unfolding procedure.³

3 Inclusive Jet Cross Section

The final measurements in each of the five $|\eta|$ regions, along with statistical uncertainties, are presented in Fig. 1b (tables of the measured cross sections can be found in³). The measurement spans about seven orders of magnitude and extends to the highest jet energies ever reached. Figure 1b also shows $\mathcal{O}(\alpha_s^3)$ theoretical predictions from JETRAD¹ with renormalization and

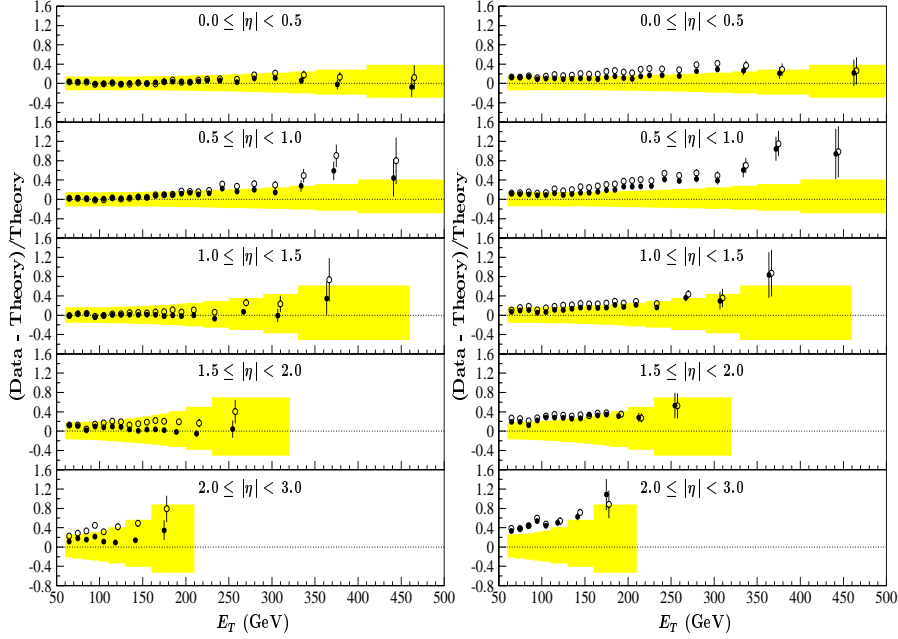


Figure 2. Comparisons between the $D\bar{O}$ single inclusive jet cross sections and the $\mathcal{O}(\alpha_s^3)$ QCD predictions calculated by JETRAD. Left panel shows comparisons with the CTEQ4HJ (\bullet) and CTEQ4M (\circ) PDFs while the right panel shows comparisons with the MRSTg \uparrow (\bullet) and MRST (\circ) PDFs. (The highest E_T points are offset slightly for CTEQ4M and MRST.)

factorization scales set to half of the E_T of the leading jet and using the CTEQ4M PDF.

Left and right panels in Fig. 2 provide more detailed comparisons to predictions on a linear scale for several PDFs (for other PDFs, see ³). The error bars are statistical, while the shaded bands indicate one standard deviation systematic uncertainties. The theoretical uncertainties due to variations in input parameters are comparable to the systematic uncertainties. These qualitative comparisons indicate that the predictions are in reasonable agreement with the data for all $|\eta|$ intervals.

To quantify the comparisons, we employ a specially derived and previously studied χ^2 statistic ^{3,7} employing all 90 η - E_T bins in this measurement, including correlations in E_T as well as in η . For all PDFs we have considered, Table 1 lists the χ^2 , χ^2/dof , and the corresponding probabilities for 90 degrees of freedom (dof). We have verified that the variations of correlation coefficients within the range of their uncertainties give a similar ordering of

Table 1. The χ^2 , χ^2/dof , and the corresponding probabilities for 90 degrees of freedom for various PDFs studied.

PDF	χ^2	χ^2/dof	Probability
CTEQ3M	121.56	1.35	0.01
CTEQ4M	92.46	1.03	0.41
CTEQ4HJ	59.38	0.66	0.99
MRST	113.78	1.26	0.05
MRSTg \downarrow	155.52	1.73	<0.01
MRSTg \uparrow	85.09	0.95	0.63

the χ^2 , hence a similar relative preference of PDFs. The absolute values of χ^2 and associated probabilities vary somewhat with variations in the correlations in E_T and, to a much lesser extent, with variations of correlations in η . The theoretical predictions are in good quantitative agreement with the experimental results. The data indicate a preference for the CTEQ4HJ, MRSTg \uparrow , and CTEQ4M PDFs. The CTEQ4HJ PDF has enhanced gluon content at large x , favored by previous measurements of inclusive jet cross sections at small η , relative to the CTEQ4M PDF. The MRSTg \uparrow PDF includes no intrinsic parton transverse momentum and therefore has effectively increased gluon distributions relative to the MRST PDF. This measurement provides the world's best constraint on the gluon distribution at high x and is being included in the new global PDF fits by the MRST and CTEQ Collaborations.

References

1. S. D. Ellis, Z. Kunszt, and D. E. Soper, Phys. Rev. Lett. **64**, 2121 (1990); F. Aversa *et al.*, Phys. Rev. Lett. **65**, 401 (1990); W. T. Giele, E. W. N. Glover, and D. A. Kosower, Phys. Rev. Lett. **73**, 2019 (1994).
2. H. L. Lai *et al.*, Phys. Rev. D **51**, 4763 (1995); Phys. Rev. D **55**, 1280 (1997); A. D. Martin *et al.*, Eur. Phys. J. C **4**, 463 (1998).
3. B. Abbott *et al.* (DØ Collaboration), Phys. Rev. Lett. **86**, 1707 (2001); L. Babukhadia, Ph.D. Dissertation, University of Arizona, Tucson, Arizona, USA 1999, <http://fnalpubs.fnal.gov/techpubs/theses.html>.
4. S. Abachi *et al.* (DØ Collaboration), Nucl. Instr. Meth. Phys. Res. A **338**, 185 (1994).
5. D.E. Groom *et al.* (Particle Data Group), Eur. Phys. J. C **15**, 1 (2000).
6. B. Abbott *et al.* (DØ Collaboration), Nucl. Instr. Meth. Phys. Res. A **424**, 352 (1999); A. Goussiou, Report No. Fermilab-Pub-99/264-E, 1999.
7. B. Abbott *et al.* (DØ Collaboration), accepted by Phys. Rev. D, hep-ex/0012046, Fermilab-Pub-00/216-E, 2000.